MicroRNA-Mediated Control of Cell Fate in Megakaryocyte-Erythrocyte Progenitors

Published as: *Dev Cell*. 2008 June ; 14(6): 843–853.

microRNA-mediated control of cell fate in megakaryocyte-erythrocyte progenitors

Jun Lu[1,2,*], **Shangqin Guo**[3,4,*], **Benjamin L. Ebert**[1,2,*], **Hao Zhang**[1], **Xiao Peng**[1], **Jocelyn Bosco**[1], **Jennifer Pretz**[1], **Rita Schlanger**[3,4], **Judy Y. Wang**[1], **Raymond H. Mak**[1], **David M. Dombkowski**[5], **Frederic I. Preffer**[5], **David T. Scadden**[3,4], and **Todd R. Golub**[1,2,6,**]

1 *Broad Institute of MIT and Harvard, Cambridge, Massachusetts 02142, USA*

2 *Department of Pediatric Oncology, Dana-Farber Cancer Institute, Harvard Medical School, Boston, Massachusetts 02115, USA*

3 *Center for Regenerative Medicine, Massachusetts General Hospital, Harvard Medical School, Boston, Massachusetts 02114, USA*

4 *Harvard Stem Cell Institute, Cambridge, Massachusetts 02138, USA*

5 *Department of Pathology, Massachusetts General Hospital, Harvard Medical School, Boston, Massachusetts 02129, USA*

6 *Howard Hughes Medical Institute*

Summary

Lineage specification is a critical issue in developmental and regenerative biology. We hypothesized that microRNAs (miRNAs) are important participants in that process and used the poorly-understood regulation of megakaryocyte-erythrocyte progenitors (MEPs) in hematopoiesis as a model system. We report here that miR-150 modulates lineage fate in MEPs. Using a novel methodology capable of profiling miRNA expression in limiting numbers of primary cells, we identify miR-150 as preferentially expressed in the megakaryocytic lineage. Through gain- and loss-of-function experiments, we demonstrate that miR-150 drives MEP differentiation toward megakaryocytes at the expense of erythroid cells *in vitro* and *in vivo*. Moreover, we identify the transcription factor *MYB* as a critical target of miR-150 in this regulation. These experiments show that miR-150 regulates MEP fate, and thus establish a role for miRNAs in lineage specification of mammalian multi-potent cells.

Introduction

Lineage specification is critical in mammalian development and in the maintenance of adult tissue. The generation of mature effector cells in any organ involves the progressive differentiation of stem cells and multi-potent progenitors into committed cells of distinct lineages. In mammals, this developmental hierarchy has been most extensively studied in the hematopoietic system, where well-characterized cell surface markers allow for the purification of distinct cell populations. Lineage specification has been thought to be largely regulated at

**Correspondence should be addressed to T.R.G (E-mail: golub@broad.mit.edu; phone: 617-252-1927; fax: 617-258-0903).
*These authors contributed equally to this work.

the level of transcription, where lineage-specific transcription factors drive specific cell fates (see reviews (Cantor and Orkin, 2002; Friedman, 2002; Ye and Graf, 2007; Zhu and Emerson, 2002)). For example, the transcription factor C/EBPα specifies neutrophilic differentiation (Friedman, 2002), and GATA-3 drives Th2 lineage commitment of CD4 T cells (Zheng and Flavell, 1997). However, differential transcription of transcription factors does not appear to explain all of hematopoietic cell fate decisions, leading to the possibility that other mechanisms exist for establishing cell fate. As an example, the process by which megakaryocyte-erythrocyte progenitors (MEPs) commit to becoming either erythroid precursors, yielding mature red blood cells, or megakaryocytes, yielding mature platelets, is unknown. Despite much effort, lineage-specific transcription factors responsible for guiding the fate of MEPs have not yet been identified.

We hypothesized that the developmental fate of mammalian multi-potent cells might be guided at least in part by a different mechanism of gene regulation, namely by miRNAs. These ~22nt non-coding RNAs negatively regulate the expression of target proteins primarily by inhibiting translation of their cognate mRNAs through sites in the 3′UTR (see review (Bartel, 2004)), and are functionally important in diverse cellular processes (Ambros, 2004; Chen et al., 2004), including the differentiation of committed cells (Fazi et al., 2005; Fontana et al., 2007; Fukao et al., 2007; Xiao et al., 2007; Zhou et al., 2007). Our previous result that miRNA expression patterns encode developmental history supports a role of miRNAs in lineage specification (Lu et al., 2005).

In this study, we used MEP differentiation as a model system to test this hypothesis. Using a novel miRNA profiling technology, we profiled miRNA expression in MEPs, erythroid and megakaryocytic primary cells and identified miR-150 with preferential expression in the megakaryocytic lineage. Gain- and loss-of-function experiments established that miR-150 regulates MEP fate to reciprocally modulate megakaryocytic and erythroid development, through antagonizing a broadly expressed and developmentally important transcription factor *MYB*. Our results elucidate an important mechanism for the poorly understood regulation of MEP fate, and establish a role of miRNAs in mammalian lineage specification.

Results

Development of a sensitive, genome-wide miRNA expression profiling technology

To study miRNAs in MEP development, we took the unbiased approach to profile the expression of miRNAs in MEPs, erythroid and megakaryocytic primary cells. Unfortunately, the small number of precursor cells obtainable from human donors has precluded a thorough analysis of miRNA expression in hematopoiesis (and other systems) using conventional miRNA profiling methods, which generally require either large amounts of input RNA, or are not amenable to genome-wide, high-throughput applications. To address this technical challenge, we developed a method in which mature miRNAs are captured in 96-well plates using immobilized 5′-amino-modified oligonucleotides complementary to the mature miRNA sequence of the more than 300 human miRNAs in miRBASE release 7.0 (Griffiths-Jones et al., 2006). This plate-based capture obviates the need for gel-purification of small RNAs which, in addition to being labor-intensive, results in significant loss of input miRNAs. The captured miRNAs were ligated with adaptors on 3′ and 5′ ends successively, reverse transcribed, and amplified via PCR (Fig. 1A). The biotinylated PCR products were then detected by hybridization to fluorescent beads coupled to capture oligonucleotides complementary to the mature miRNA sequence. The beads were then analyzed by flow cytometry, where the color of the bead indicates the identity of the miRNA and the phycoerythrin channel indicates the abundance of that particular miRNA (Lu et al., 2005). In contrast to our previously reported method that required ~ 10 μg of input RNA (Lu et al., 2005), the present method yields similarly

informative results with as little as 10 ng of total RNA (Fig. S1), allowing us to profile miRNA expression in rare cell populations.

The differential expression of miR-150 supports a role in MEP fate specification

With a suitable miRNA profiling method in hand, we examined the miRNA expression pattern in MEPs and early megakaryocytic and erythroid populations obtained from FACS-sorted human umbilical cord blood samples. Using well-established surface markers, we purified 6 populations of cells, and refer to them as MEP (*CD34*$^+$,*CD38*$^+$,*IL-3R α*$^-$,*CD45RA*$^-$), MEGA1 (*CD34*$^+$,*CD41*$^+$,*CD61*$^+$,*CD45*$^-$), MEGA2 (*CD34*$^-$,*CD41*$^+$,*CD61*$^+$,*CD45*$^-$), ERY1 (*CD34*$^+$,*CD71*$^+$,*GlyA*$^-$), ERY2 (*CD34*$^-$,*CD71*$^+$,*GlyA*$^-$) and ERY3 (*CD34*$^-$,*CD71*$^+$,*GlyA*$^+$). These 6 populations thus capture the bifurcation of the megakaryocytic and erythroid lineages with fine granularity (Fig. 1C).

Profiling of 320 miRNAs was performed to identify those most differentially expressed across the human megakaryocytic and erythroid populations (Fig. 1B, Table S4). For example, miR-451 and miR-144 were highly expressed in CD71$^+$GlyA$^+$ erythrocytes, and miR-222 was downregulated during erythropoiesis as previously described (Felli et al., 2005;Zhan et al., 2007) (Fig. 1B). Differential analysis unexpectedly identified miR-150, previously thought to be lymphocyte-specific (Zhou et al., 2007), with the most divergent expression between early megakaryocytic and erythroid cells, being expressed > 15-fold higher in megakaryocytes (Fig. 1C, Table S1). Quantitative RT-PCR analysis in sorted umbilical cord blood cells confirmed miR-150 as being highly expressed in megakaryocytes, weakly expressed in erythrocytes and moderately expressed in MEPs (Fig. 1D, S2). Similarly, miR-150 was expressed more highly in CD41$^+$CD61$^+$ megakaryocytes than in CD71$^+$GlyA$^+$ erythrocytes in human adult bone marrow (Fig. 1E).

In addition to differential expression, miR-150 displays exquisite sequence conservation across organisms with functional erythrocytic and thrombocytic systems, exhibiting identical sequence in the 5′ seed region that mediates target recognition (Fig. S3). Together, these evidences support the hypothesis that miR-150 regulates lineage specification in MEPs.

miR-150 reciprocally regulates megakaryocyte and erythrocyte development *in vitro* and *in vivo*

To assess a potential causal role of miR-150 in the specification of megakaryocytes versus erythrocytes, we performed a series of *in vitro* and *in vivo* experiments.

First, we used a bi-lineage primary cell culture system, in which human CD34$^+$ hematopoietic progenitor cells isolated from adult human bone marrow, when cultured in the presence of thrombopoietin and erythropoietin, differentiate along the megakaryocytic and erythroid lineages *in vitro* (Fig. 2A). This system allowed us to quantitate the proportion of megakaryocytic and erythroid cells derived from progenitors following perturbation of miR-150. We transduced CD34$^+$ cells with a lentiviral construct harboring miR-150, resulting in a physiological level of miR-150 expression that is similar to that observed in primary megakaryocytes (Fig. S4). Megakaryocytes were then enumerated by flow cytometry measuring the CD41$^+$GlyA$^-$ population. Compared to CD34$^+$ cells transduced with a control vector (shLuc, expressing a short hairpin RNA against luciferase), the miR-150 expressing cells yielded an average of 8-fold enrichment of megakaryocytes (Fig. 2B, 2C). In contrast, mutant miR-150, or an irrelevant miRNA construct (miR-15b-16-2), did not produce significant increase in megakaryocytes. This result indicates that miR-150 shifts the balance of megakaryocytic-erythroid differentiation towards megakaryocytes, and further suggests its role in governing the fate of MEPs.

Having established a functionally important role of miR-150 in a human *in vitro* model of MEP differentiation, we next examined the function of miR-150 *in vivo*. To this end, we used a murine bone marrow transplant model, in which stem/progenitor-cell-enriched bone marrow cells from donor mice were transduced with either miR-150 retrovirus or control virus, and the cells then transplanted into lethally irradiated syngeneic recipient mice (Fig. 3A). Both viral vectors carry GFP as a marker, allowing us to distinguish between donor-derived cells that were transduced from those that were not. To avoid early lethality of transplant recipients due to possible impact on the erythroid lineage and to avoid potential secondary compensatory mechanism, we used low viral titer that resulted in ~20% transduction efficiency.

Using flow cytometry, we assayed the bone marrow cells with megakaryocyte- (CD41) and erythrocyte- (Ter119) specific markers. Strikingly, compared to either non-transduced (GFP^-) cells in miR-150 recipients, or vector control recipient mice, miR-150 transduced (GFP^+) bone marrow cells exhibited a dramatic (> 15-fold on average) expansion of megakaryocytes ($CD41^+Ter119^-$) in relation to all transduced cells in the bone marrow (Fig. 3B, 3D, S5). In addition, we observed a strong elevation in the expression of the megakaryocyte-specific gene PF4 (Ravid et al., 1991) in miR-150 transduced bone marrow cells (Fig. 3E), and observed a consistent 2- to 14-fold enrichment in GFP^+ circulating platelets in miR-150 animals compared to control (Fig. 3F, S6). These results proved that miR-150 expression led to an increase in bone marrow megakaryocytes that were competent to produce mature platelets in circulation.

In contrast, forced expression of miR-150 led to a >60% *decrease* in GFP^+ erythrocytes ($Ter119^+CD41^-$), coupled with an *increase* in GFP^+ megakaryocytes in the bone marrow, both in percentage and in cell number (Fig. 3C, 3D, S7). We further examined bone marrow cells with CD71 and Ter119, which distinguish different stages of murine erythroid differentiation (Socolovsky et al., 2001). The R1 to R4 gates on CD71/Ter119 plot show that miR-150 expressing cells displayed a strong shift toward an immature state, compared to controls (Fig. 3G,3H,3I). Specifically, miR-150 expression led to an average of 8-fold increase in the immature R1 population, and a more than 60% decrease in the late R4 stage. These experiments indicate that ectopic miR-150 expression induces a block in the earliest definable stage of murine adult erythropoiesis, in addition to causing a significant reduction in the total erythroid population.

These *in vitro* and *in vivo* experiments showed that miR-150 reciprocally regulates megakaryocytic and erythroid development, further supporting a role of miR-150 in lineage specification of MEPs.

miR-150 regulates lineage fate in MEPs

We next asked whether the megakaryocyte-promoting effect of miR-150 was due to its effect on MEP commitment, or was simply an effect on post-commitment megakaryocytic proliferation or survival. To address this, we used a colony formation assay to quantitate the megakaryocytic potential of progenitor cells at the single cell level. We found that miR-150 forced expression resulted in a statistically significant increase in megakaryocyte colony-forming units (CFU-Mk) in transduced bone marrow cells (Fig. 4A), coupled with a dramatic decrease in erythroid colony formation (Fig. 4B,4F). These gain-of-function experiments strongly suggest that miR-150 regulates MEP fate, and not simply post-commitment megakaryocyte expansion.

To complement these miR-150 forced expression studies, we turned to a loss-of-function approach. MEP cells were purified from bone marrow, and assayed for megakaryocyte colony formation in the presence or absence of an antagomir (a cholesterol-modified antisense oligonucleotide (Krutzfeldt et al., 2005)) directed against miR-150. Antagomir-150, but not a

scrambled control, successfully knocked down miR-150 expression. (Fig. 4E). MEPs treated with antagomir-150 showed more than a 4-fold decrease in CFU-Mk, compared to vehicle or a scrambled antagomir (Fig. 4C). A similar effect was observed using purified uncommitted $Lin^{-}Kit^{+}Sca^{+}$ hematopoietic stem cells (Fig. 4D). Interestingly, miR-150 knock-down megakaryocyte colonies showed normal morphology and acetylcholinesterase activity (Fig. 4G), suggesting that miR-150 is dispensable once MEP commitment to the megakaryocyte lineage is established.

Having established a role of miR-150 in regulating MEP fate, we reasoned that miR-150 expression may be regulated in progenitor cells under physiologic challenge. We treated mice with the anemia-inducing drug phenylhydrazine, and then measured miR-150 expression in lineage-negative bone marrow cells, which preceded evidence of erythroid differentiation.miR-150 expression was significantly decreased in this setting of increased demand for erythropoiesis (Fig. 4H). These data are consistent with miR-150's role in promoting megakaryopoiesis at the expense of erythropoiesis, and its alteration under a physiologic challenge, such as anemia.

MYB is a functional target of miR-150

The experiments described above firmly establish an important role of miR-150 in the specification of megakaryocytes from MEPs. We next sought to determine the mRNA targets of miR-150 that explain its effect on megakaryocytic/erythroid outcome. We started with the targets predicted in common among several sequence-based prediction algorithms (Krek et al., 2005; Lewis et al., 2005; Xie et al., 2005). We focused further on *MYB* (also known as *c-myb*) as a candidate because several recently reported mouse models, in which *MYB* activity was reduced due to either mutation or the serendipitous integration of a transgene near the *MYB* locus, displayed thrombocytosis and anemia (Emambokus et al., 2003; Kasper et al., 2002; Mucenski et al., 1991; Mukai et al., 2006; Sandberg et al., 2005). The expression of *MYB* messenger RNA, however, is not immediately suggestive of a role in MEP differentiation, as we observed similar expression in MEPs and early erythroid and megakaryocyte populations (Fig. S8). Examination of the human *MYB* 3′UTR, however, identified multiple conserved miR-150 putative binding sites (Fig. S9).

To establish miR-150 as a functional negative regulator of *MYB*, we first studied the human erythroblastic cell line K562 and the murine hematopoietic progenitor cell line EML-1, both of which have the potential to be induced to differentiate into erythroid or megakaryocytic cells. We observed a dramatic reduction in *MYB* protein level upon ectopic expression of miR-150 (Fig. 5A, S10). Next, we cloned the *MYB* 3′ UTR into a luciferase reporter, and found that miR-150 repressed reporter activity by more than 6-fold, again consistent with miR-150 targeting *MYB*. Importantly, mutation of the 4 candidate miR-150 binding sites abrogated miR-150 repression, and a mutant miR-150 construct designed to be complementary to the mutant *MYB* 3′UTR binding sites restored miR-150 mediated repression, but did not affect the wild-type *MYB* 3′UTR (Fig. 5B, 5C). These experiments establish that miR-150 negatively regulates the protein level of *MYB* directly through its 3′ UTR.

Lastly, we addressed whether miR-150 repression of *MYB* explains miR-150's erythroid/megakaryocytic effects. We tested this hypothesis using the *in vitro* $CD34^{+}$ human bone marrow cell culture. Consistent with reports that mice with reduced *MYB* activity develop megakaryocytosis (Emambokus et al., 2003; Kasper et al., 2002; Mucenski et al., 1991; Mukai et al., 2006; Sandberg et al., 2005), two independent shRNA constructs that knocked down *MYB* expression promoted megakaryocyte development (Fig. 5D,5E). In contrast, forced expression of a *MYB* cDNA construct lacking its 3′UTR resulted in a decrease in megakaryocytes (Fig. 4F,4G). Moreover, the *MYB* expression construct rescued the

megakaryocyte-promoting effect of miR-150, indicating that *MYB* is a functionally relevant downstream effector of miR-150 (Fig. 4F,4G).

Discussion

The work here demonstrates for the first time that miRNAs play an important role in the developmental fate regulation of multi-potent progenitor cells in mammals. Our results challenge the view that miRNAs play merely fine-tuning roles in establishing lineage fate (Bartel, 2004; Li et al., 2006). The function of miR-150 demonstrated here provides some of the first insights into the regulation of MEP fate decision, about which very little is known. Our studies, of course, do not exclude the possibility that additional factors may also contribute to the establishment of MEP fate.

Future investigations may use miR-150 as a tool to dissect the details of extracellular and intracellular pathways that are involved in MEP lineage specification. Furthermore, exploring the regulation of miR-150 expression is also likely to be fruitful. Both transcriptional and post-transcriptional mechanisms exist for modulating miRNA expression (Chang et al., 2008; Thomson et al., 2006). Thus, mapping the transcriptional start site of miR-150, understanding its promoter elements and investigating possible post-transcriptional control would shed light on the regulation of miR-150 expression. We explored the possibility that a feedback loop of *MYB* regulating miR-150 expression might be utilized, but we saw no evidence of this in either SupT11 or K562 cells (data not shown).

Identifying *MYB* as a functional target of miR-150 is consistent with a recent study showing MEPs with reduced *MYB* activity favor megakaryocytic as opposed to erythroid differentiation (Mukai et al., 2006). In contrast to total loss of *MYB* function, which results in complete hematopoietic failure (Mucenski et al., 1991), our data indicate that modest modulation of *MYB* expression levels by miR-150 can have important effects on lineage specification. These results are particularly interesting in light of the recent report of miR-150 regulation of *MYB* activity in B-lineage lymphocytes (Xiao et al., 2007). It has been generally assumed that miRNAs have a plethora of targets that vary depending on cellular context. Remarkably, *MYB* appears to be a critical target of miR-150 both in establishing MEP fate and in regulating the differentiation of lineage-committed B-cells. This observation suggests that a single mRNA target of a miRNA might explain much of the miRNA's function, even in completely different developmental contexts. Our results, however, do not exclude the possibility that other miR-150 targets may be involved in establishing or maintaining MEP fate decision. For example, *pim-1*, a predicated target of miR-150, is known to positively regulate *MYB* (Leverson et al., 1998), suggesting that miR-150 may suppress multiple genes in the *MYB* pathway. In addition, miR-150 is predicated to target several genes associated with epigenetic regulation, which could play a role in lineage specification. Further experiments are clearly needed to test these hypotheses.

The miR-150/*MYB* mechanism may explain in part why a search for lineage-specific expression of transcription factors or other regulators has failed to identify key modulators of MEP differentiation. Indeed, miR-150 is not megakaryocyte-specific; it is also abundantly expressed in lymphoid cells (Xiao et al., 2007; Zhou et al., 2007). Similarly, *MYB* expression is not specific to the erythroid and megakaryocytic lineages, but rather it is broadly expressed in hematopoiesis and beyond (Ramsay et al., 2003). This observation suggests a mechanism by which an exquisitely lineage-specific developmental program can be executed through the combinatorial expression of a miRNA and a transcription factor at the critical junction of lineage fate specification. Given the large number of fate decisions required for mammalian development, we speculate that similar miRNA/transcription factor mechanisms are utilized

in other developmental settings. It is also conceivable that manipulation of specific miRNAs to influence stem and progenitor cell fate might have therapeutic value.

Experimental Procedures

miRNA expression profiling and data analysis

miRNA expression profiling was performed using the plate capture method unless otherwise stated. 96-well PCR plates with N-oxysuccinimide surface (DNA-BIND plates, Corning Costar) were coated at room temperature for 1 hour with 5 μM mixture of 5′ amino-antisense oligonucleotides (see Table S2) at 20 μl per well according to manufacturer's protocol. Coated plates were successively washed with (100 mM Tris-HCl, pH8.0, 150 mM NaCl, 1 mM EDTA) and (10 mM Tris-HCl, pH 8.0, 1 mM EDTA). Total RNA (10 ng or higher) was diluted to 20 μl in 50 mM Tris-HCl, pH 8.0, 1 M NaCl, 1 mM EDTA, 1x RNAsecure (Ambion), containing pre-control synthetic miRNA mixture at the ratio previously described (Lu et al., 2005). miRNAs were captured in the coated wells by denaturing at 80 °C for 5 minutes and gradually cooling to room temperature in 1.5 hours in a PCR machine, followed by three 2xSSC washes. 3′ adaptor ligation and 5′ adaptor ligations were carried out as described (Lu et al., 2005) in 20 μl reaction volumes, with four 2xSSC washes after each ligation. Ligated miRNA were denatured for 5 minutes at 80 °C in 20 μl water with 2 μM adaptor-specific RT primer, chilled on ice, and reverse transcribed as described (Lu et al., 2005). RT products were denatured at 95 °C for 5 minutes before 2 rounds of PCR amplification with described conditions (Lu et al., 2005), for 26 and 27 cycles respectively, to incorporate biotin labels for low input RNA profiling. Labeled miRNAs were hybridized to a bead-based detection platform (Lu et al., 2005), with updated detection probes (Table S3). Median fluorescence intensities were quantitated on a Luminex 100S machine (Luminex Corp).

Data were normalized as described (Lu et al., 2005) with modifications. Average readings from 5 water-only labeled samples were used for probe-specific background subtraction. Linear normalization among different bead sets for the same sample was performed using readings from 2 post-control probes with equal contribution. Sample normalization was subsequently carried out assuming equal total fluorescence readings. To identify markers, all ERY samples were compared to all MEGA samples, with median-based t-test and 50,000 permutations, using the ComparativeMarkerSelection module in GenePattern (Reich et al., 2006).

Cell sorting and flow cytometry

Human umbilical cord blood was harvested at Brigham and Women's Hospital with informed patient consent under an IRB approved protocol. Adult human bone marrow cells were obtained from AllCells, LLC. Mononuclear cells were purified by Ficoll Hypaque sedimentation. Lineage depletion was performed using antibodies against CD2, CD3, CD4, CD5, CD8, CD11b, CD14C, CD19, and CD56 with a magnetic column (Miltenyi Biotec). Populations were defined as follows: MEP ($CD34^+CD38^+IL\text{-}3Ra^-CD45RA^-$), ERY1 ($CD34^+CD71^+GlyA^-$), ERY2 ($CD34^-CD71^+GlyA^-$), ERY3 ($CD34^-CD71^+GlyA^+$). Megakaryocytes were purified without lineage depletion according to the following immunophenotypes: MEGA1 ($CD34^+CD61^+CD41^+CD45^-$), MEGA2 ($CD34^-CD61^+CD41^+CD45^-$). Adult human bone marrow cells were similarly sorted according to $CD34^-CD61^+CD41^+$ and $CD34^-CD71^+GlyA^+$. Sorting was performed with a Vantage SE Diva or with an Aria (BD Biosciences). RNA was extracted using TriZol (Invitrogen).

For the *in vitro* human primary culture experiment, approximately 500,000 cells were stained with CD41-FITC, Ter119-PE and CD71-PE-Cy5 antibodies for 15 minutes on ice and washed twice before flow cytometry. For analysis of transplant recipients, murine bone marrow cells

were labeled with CD41-PE and Ter119-APC, or Ter119-APC and CD71-PE. Peripheral blood cells were harvested into 0.38% sodium citrate and stained with CD41-PE.

Mouse MEPs were purified as described in (Akashi et al., 2000). Briefly, bone marrow cells were harvested from 8- to 10-week old C57Bl6/J mice and stained with a lineage antibody cocktail containing biotinylated lineage markers including Ter119, CD3, CD4, CD8, CD11b/Mac-1, Gr-1 and B220, and followed by staining with a second antibody cocktail containing streptavidin-PerCP, Sca-PE, cKit-APC, CD16/32 PE-Cy7 and CD34-PacificBlue. MEPs are defined as the $Lin^{-}cKit^{+}Sca^{-}CD34^{-}CD16/32^{-}$ population.

Refer to the antibody section in Supplemental Data for antibodies used.

Constructs

Constructs were prepared with standard molecular biology techniques. Details of plasmids and their construction are available in Supplemental Data.

Quantitative RT-PCR

Quantitative RT-PCR for miRNAs or mRNAs were performed using assays from Applied Biosystems on an ABI HT7900 real time PCR machine. Data were normalized with 18S ribosomal RNA readings. ΔCt values (Ct of 18S minus Ct of gene of interest) were used unless specified otherwise. Details are available in Supplemental Data.

In vitro primary culture of human $CD34^{+}$ cells

Cryopreserved human adult bone marrow $CD34^{+}$ cells were obtained from Cambrex (Poietics; Cambrex). Cells were cultured in Serum Free Expansion Medium (SFEM, Stem Cell Technologies) supplemented with 100 U/mL penicillin/streptomycin, 2 mM glutamine, and 40 μg/mL lipids (Sigma). Erythroid and megakaryocytic differentiation were supported in a single liquid culture, similarly as described (Ebert et al., 2005), in the presence of 50 ng/mL TPO, 100 ng/mL SCF, 10 ng/mL IL-3, 10 ng/mL IL-6, and 0.5 U/mL EPO. The concentration of EPO was increased to 3 IU/mL on day 7. Cells were harvested for flow cytometry following 10 days of liquid culture. Lentiviral infection was performed starting one day after thawing cells. Where indicated, cDNA construct and miRNA construct were infected on consecutive days. Cells were selected with 2 μg/mL puromycin and/or 3μg/mL blasticidin one day after infection.

Murine bone marrow transplant

All mice were purchased from the Jackson Laboratory. Murine bone marrow transplant was performed similarly as previously described (Stier et al., 2002), and approved by the MGH Subcommittee on Research Animal Care. Donor C57Bl6/J mice (~8 weeks) were primed with 150 mg/kg 5FU for four days. Bone marrow cells were purified by Ficoll (GE Healthcare) density gradient centrifugation, following the manufacturer's protocol. Cells were transduced with empty vector or miR-150 retrovirus in X-VIVO 15 medium (Biowhittaker) supplemented with 100 ng/mL SCF, 50 ng/mL TPO, 50 ng/mL Flt3 ligand and 20 ng/mL IL3 by centrifugation onto plates coated with retronectin (Takara). To avoid possible early lethality of transplant recipients due to the negative effect of miR-150 on erythroid differentiation, and to avoid possible organismal compensatory effects, a low titre of virus was used, producing ~20% transduction efficiency for both vector control and miR-150 constructs. Lethally irradiated (9.5 Gy) recipient mice were transplanted with 2.5–4 million cells the day after infection. Hematopoietic recovery was monitored by complete blood count. Bone marrow cells of recipients were analyzed at 5 to 8 weeks post-transplantation. Platelets were analyzed 7-weeks post-transplantation.

Cell culture

K562 and 293T cells were obtained from ATCC, and were cultured according to ATCC instructions. SupT11 was a kind gift from Dr. Gary Gilliland. EML-1 cells were cultured in IMDM, supplemented with 20% horse serum and 20% BHK/MKL-conditioned medium. Transfection was performed using FuGENE6 (Roche). Retro- or lenti-virus was produced in 293T cells following standard procedures.

Mouse bone marrow cells were treated with antagomir (50 μg/ml) or PBS for three days in X-VIVO 15 medium (Biowhittaker) supplemented with 50 ng/mL SCF, 50 ng/mL TPO, 50 ng/mL Flt3 ligand and 20 ng/mL IL3. Cells were then harvested for RNA analysis.

Oligonucleotides and antagomirs

DNA oligonucleotides were synthesized by IDT Technology. RNA oligonucleotides, including antagomirs and DNA-RNA hybrids, were synthesized by Dharmacon. Antagomir stock solution was prepared in PBS. Antagomir-150: 5′ mC(*)mA(*) mCmUmGmGmUmAmCmAmAmGmGmGmUmUmGmGmG(*)mA(*)mG (*)mA (*)(3′-Chl) 3′. Antagomir-scrambled: 5′mC(*)mU(*)mCmGmCmGmUmAmGmA mAmGmAmGmUmAmGmGmU(*)mG(*)mG(*)mA(*) (3′-Chl) 3′. (mN: 2′OMe base; *: phosphorothioate linkage; Chl: cholesterol).

Colony assay

Megakaryocyte colony assay was performed using the MegaCult-C kit (Stem Cell Technology) according to the manufacturer's protocol. Bone marrow cells from recipient mice 7 to 10 weeks after transplantation were sorted into GFP− and GFP+ populations. Two recipient mice were analyzed for each construct, and each population of cells was assayed in duplicates with 100,000 sorted bone marrow cells per well. Cultures were maintained for 8 days before stained for acetylcholinesterase activity and scored. For antagomir treatment, 1000 LKS cells or 4000 MEPs were FACS-sorted and assayed in the presence of antagomir (50 μg/ml) or PBS and maintained in culture for 11 days before staining and scoring. In all cases, a colony with ≥3 acetylcholinesterase-positive cells was scored as a megakaryocyte colony.

For erythroid colony assay, 5FU primed wild type C57Bl6/J marrow was transduced as described above. Forty-eight hours after viral transduction, 30,000 GFP+ cells were FACS-sorted and plated into methylcellulose (StemCell Technologies, M3334) which only contains EPO.

Anemic response

Phenylhydrazine hydrochloride (Sigma) solution in PBS was injected intraperitoneally into 10- to 12-week wild type C57Bl6/J mice (60 mg/kg body weight) on each of days 0, 1, and 2. On the 3rd day, mice were euthanized by CO_2 inhalation and bone marrow was harvested and stained with a lineage marker antibody cocktail as described in cell sorting and flow cytometry. Lineage negative cells were FACS sorted into TriZol reagent for RNA preparation.

Western blot analysis

Western blot analysis was performed as previously described (Lu et al., 2004). Cells were infected with retroviral constructs and selected with puromycin for two days before harvesting. *MYB* antibody (clone 1-1) was from Upstate Biotechnology. Beta tubulin antibody (ab6046) was from Abcam.

Luciferase reporter assay

293T cells were plated in 96 well plates at 5000 cells per well the day before transfection. Transfection was carried out in 8 replicates using FuGENE 6 (Roche), with 100 ng of plasmid mixture (90 ng of expression vector and 10 ng of reporter vector in the psiCHECK2 backbone). Luciferase assays for both firefly and renilla luciferase were performed 2 days after transfection, using the Dual-Glo Luciferase assay kit (Promega). Luminescence was quantitated on a Tecan Spectrafluor Plus machine. Renilla luciferase readings were normalized against the firefly luciferase activity in the corresponding well.

Statistical Analysis

Student's t-test (2 tailed, unequal variance) was used for statistical analysis on experiments, unless otherwise specified.

Expression Data

microRNA expression data have been submitted to the Gene Expression Omnibus (GEO; http://www.ncbi.nlm.nih.gov/geo) in series GSE10593. Data are also available at http://broad.mit.edu/cancer/pub/megamiR.

Supplementary Material

Refer to Web version on PubMed Central for supplementary material.

Acknowledgments

We thank Stuart Orkin, David Kuter, Katya Ravid and Louise Purton for valuable discussions. We thank Robert Horvitz and Channing Yu for critically reading the manuscript. T.R.G. is Investigator of the Howard Hughes Medical Institute. The authors declare no competing financial interests.

References

Akashi K, Traver D, Miyamoto T, Weissman IL. A clonogenic common myeloid progenitor that gives rise to all myeloid lineages. Nature 2000;404:193–197. [PubMed: 10724173]

Ambros V. The functions of animal microRNAs. Nature 2004;431:350–355. [PubMed: 15372042]

Bartel DP. MicroRNAs: genomics, biogenesis, mechanism, and function. Cell 2004;116:281–297. [PubMed: 14744438]

Cantor AB, Orkin SH. Transcriptional regulation of erythropoiesis: an affair involving multiple partners. Oncogene 2002;21:3368–3376. [PubMed: 12032775]

Chang TC, Yu D, Lee YS, Wentzel EA, Arking DE, West KM, Dang CV, Thomas-Tikhonenko A, Mendell JT. Widespread microRNA repression by Myc contributes to tumorigenesis. Nat Genet 2008;40:43–50. [PubMed: 18066065]

Chen CZ, Li L, Lodish HF, Bartel DP. MicroRNAs modulate hematopoietic lineage differentiation. Science 2004;303:83–86. [PubMed: 14657504]

Ebert BL, Lee MM, Pretz JL, Subramanian A, Mak R, Golub TR, Sieff CA. An RNA interference model of RPS19 deficiency in Diamond-Blackfan anemia recapitulates defective hematopoiesis and rescue by dexamethasone: identification of dexamethasone-responsive genes by microarray. Blood 2005;105:4620–4626. [PubMed: 15755903]

Emambokus N, Vegiopoulos A, Harman B, Jenkinson E, Anderson G, Frampton J. Progression through key stages of haemopoiesis is dependent on distinct threshold levels of c-Myb. Embo J 2003;22:4478–4488. [PubMed: 12941699]

Fazi F, Rosa A, Fatica A, Gelmetti V, De Marchis ML, Nervi C, Bozzoni I. A minicircuitry comprised of microRNA-223 and transcription factors NFI-A and C/EBPalpha regulates human granulopoiesis. Cell 2005;123:819–831. [PubMed: 16325577]

Felli N, Fontana L, Pelosi E, Botta R, Bonci D, Facchiano F, Liuzzi F, Lulli V, Morsilli O, Santoro S, et al. MicroRNAs 221 and 222 inhibit normal erythropoiesis and erythroleukemic cell growth via kit receptor down-modulation. Proc Natl Acad Sci U S A 2005;102:18081–18086. [PubMed: 16330772]

Fontana L, Pelosi E, Greco P, Racanicchi S, Testa U, Liuzzi F, Croce CM, Brunetti E, Grignani F, Peschle C. MicroRNAs 17-5p-20a-106a control monocytopoiesis through AML1 targeting and M-CSF receptor upregulation. Nat Cell Biol 2007;9:775–787. [PubMed: 17589498]

Friedman AD. Transcriptional regulation of granulocyte and monocyte development. Oncogene 2002;21:3377–3390. [PubMed: 12032776]

Fukao T, Fukuda Y, Kiga K, Sharif J, Hino K, Enomoto Y, Kawamura A, Nakamura K, Takeuchi T, Tanabe M. An evolutionarily conserved mechanism for microRNA-223 expression revealed by microRNA gene profiling. Cell 2007;129:617–631. [PubMed: 17482553]

Griffiths-Jones S, Grocock RJ, van Dongen S, Bateman A, Enright AJ. miRBase: microRNA sequences, targets and gene nomenclature. Nucleic Acids Res 2006;34:D140–144. [PubMed: 16381832]

Kasper LH, Boussouar F, Ney PA, Jackson CW, Rehg J, van Deursen JM, Brindle PK. A transcription-factor-binding surface of coactivator p300 is required for haematopoiesis. Nature 2002;419:738–743. [PubMed: 12384703]

Krek A, Grun D, Poy MN, Wolf R, Rosenberg L, Epstein EJ, MacMenamin P, da Piedade I, Gunsalus KC, Stoffel M, et al. Combinatorial microRNA target predictions. Nat Genet 2005;37:495–500. [PubMed: 15806104]

Krutzfeldt J, Rajewsky N, Braich R, Rajeev KG, Tuschl T, Manoharan M, Stoffel M. Silencing of microRNAs in vivo with ‘antagomirs’. Nature 2005;438:685–689. [PubMed: 16258535]

Leverson JD, Koskinen PJ, Orrico FC, Rainio EM, Jalkanen KJ, Dash AB, Eisenman RN, Ness SA. Pim-1 kinase and p100 cooperate to enhance c-Myb activity. Mol Cell 1998;2:417–425. [PubMed: 9809063]

Lewis BP, Burge CB, Bartel DP. Conserved seed pairing, often flanked by adenosines, indicates that thousands of human genes are microRNA targets. Cell 2005;120:15–20. [PubMed: 15652477]

Li Y, Wang F, Lee JA, Gao FB. MicroRNA-9a ensures the precise specification of sensory organ precursors in Drosophila. Genes Dev 2006;20:2793–2805. [PubMed: 17015424]

Lu J, Getz G, Miska EA, Alvarez-Saavedra E, Lamb J, Peck D, Sweet-Cordero A, Ebert BL, Mak RH, Ferrando AA, et al. MicroRNA expression profiles classify human cancers. Nature 2005;435:834–838. [PubMed: 15944708]

Lu J, Pazin MJ, Ravid K. Properties of ets-1 binding to chromatin and its effect on platelet factor 4 gene expression. Mol Cell Biol 2004;24:428–441. [PubMed: 14673175]

Mucenski ML, McLain K, Kier AB, Swerdlow SH, Schreiner CM, Miller TA, Pietryga DW, Scott WJ Jr, Potter SS. A functional c-myb gene is required for normal murine fetal hepatic hematopoiesis. Cell 1991;65:677–689. [PubMed: 1709592]

Mukai HY, Motohashi H, Ohneda O, Suzuki N, Nagano M, Yamamoto M. Transgene insertion in proximity to the c-myb gene disrupts erythroid-megakaryocytic lineage bifurcation. Mol Cell Biol 2006;26:7953–7965. [PubMed: 16940183]

Ramsay RG, Barton AL, Gonda TJ. Targeting c-Myb expression in human disease. Expert Opin Ther Targets 2003;7:235–248. [PubMed: 12667100]

Ravid K, Beeler DL, Rabin MS, Ruley HE, Rosenberg RD. Selective targeting of gene products with the megakaryocyte platelet factor 4 promoter. Proc Natl Acad Sci U S A 1991;88:1521–1525. [PubMed: 1899930]

Reich M, Liefeld T, Gould J, Lerner J, Tamayo P, Mesirov JP. GenePattern 2.0. Nat Genet 2006;38:500–501. [PubMed: 16642009]

Sandberg ML, Sutton SE, Pletcher MT, Wiltshire T, Tarantino LM, Hogenesch JB, Cooke MP. c-Myb and p300 regulate hematopoietic stem cell proliferation and differentiation. Dev Cell 2005;8:153–166. [PubMed: 15691758]

Socolovsky M, Nam H, Fleming MD, Haase VH, Brugnara C, Lodish HF. Ineffective erythropoiesis in Stat5a(−/−)5b(−/−) mice due to decreased survival of early erythroblasts. Blood 2001;98:3261–3273. [PubMed: 11719363]

Stier S, Cheng T, Dombkowski D, Carlesso N, Scadden DT. Notch1 activation increases hematopoietic stem cell self-renewal in vivo and favors lymphoid over myeloid lineage outcome. Blood 2002;99:2369–2378. [PubMed: 11895769]

Thomson JM, Newman M, Parker JS, Morin-Kensicki EM, Wright T, Hammond SM. Extensive post-transcriptional regulation of microRNAs and its implications for cancer. Genes Dev 2006;20:2202–2207. [PubMed: 16882971]

Xiao C, Calado DP, Galler G, Thai TH, Patterson HC, Wang J, Rajewsky N, Bender TP, Rajewsky K. MiR-150 Controls B Cell Differentiation by Targeting the Transcription Factor c-Myb. Cell 2007;131:146–159. [PubMed: 17923094]

Xie X, Lu J, Kulbokas EJ, Golub TR, Mootha V, Lindblad-Toh K, Lander ES, Kellis M. Systematic discovery of regulatory motifs in human promoters and 3′ UTRs by comparison of several mammals. Nature 2005;434:338–345. [PubMed: 15735639]

Ye M, Graf T. Early decisions in lymphoid development. Curr Opin Immunol 2007;19:123–128. [PubMed: 17306518]

Zhan M, Miller CP, Papayannopoulou T, Stamatoyannopoulos G, Song CZ. MicroRNA expression dynamics during murine and human erythroid differentiation. Exp Hematol 2007;35:1015–1025. [PubMed: 17588470]

Zheng W, Flavell RA. The transcription factor GATA-3 is necessary and sufficient for Th2 cytokine gene expression in CD4 T cells. Cell 1997;89:587–596. [PubMed: 9160750]

Zhou B, Wang S, Mayr C, Bartel DP, Lodish HF. miR-150, a microRNA expressed in mature B and T cells, blocks early B cell development when expressed prematurely. Proc Natl Acad Sci U S A. 2007

Zhu J, Emerson SG. Hematopoietic cytokines, transcription factors and lineage commitment. Oncogene 2002;21:3295–3313. [PubMed: 12032771]

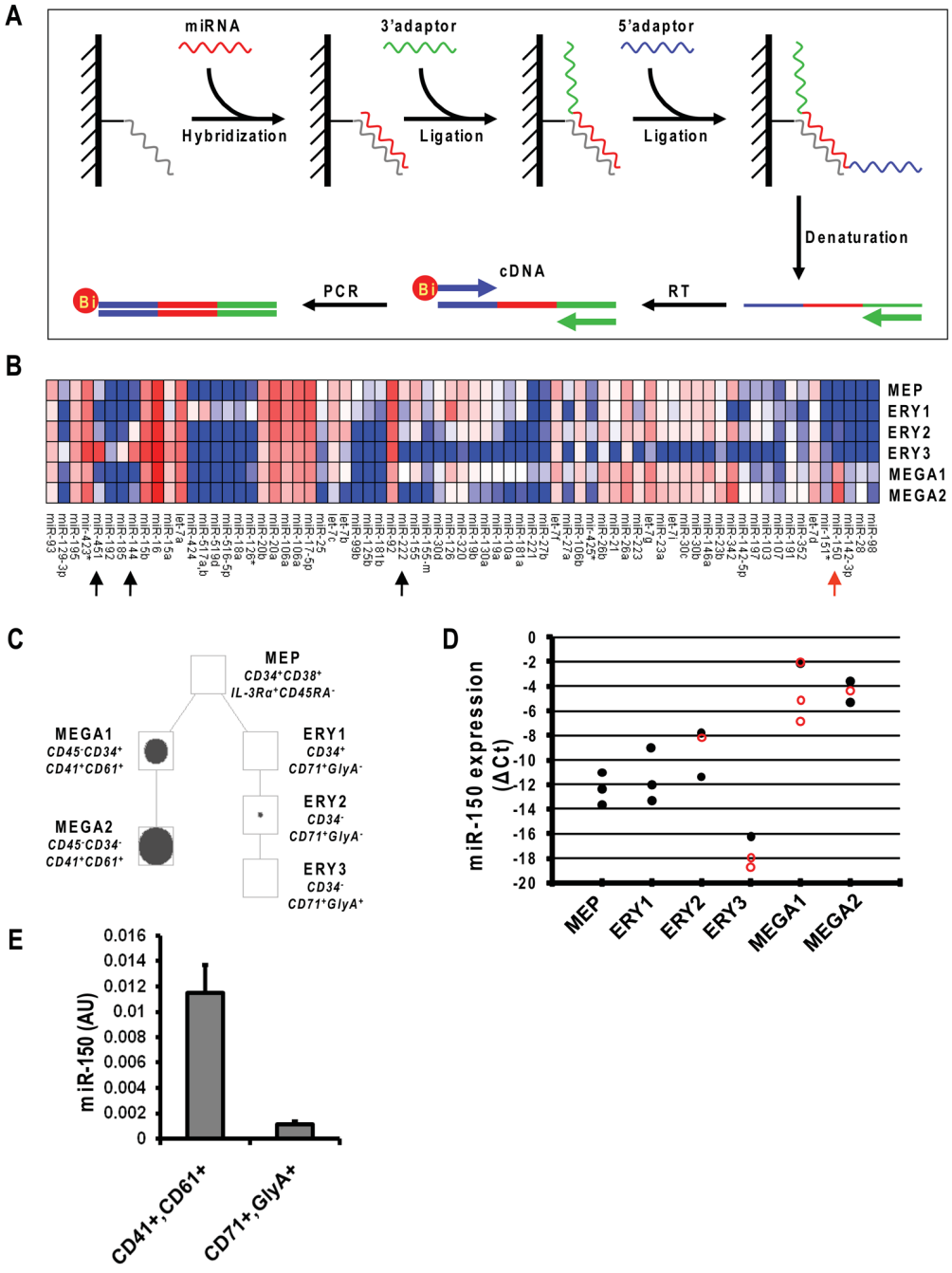

Figure 1. A novel miRNA expression profiling method identified miR-150 as being preferentially expressed in megakaryocytes

(A) Schematic of a novel, sensitive and high-throughput miRNA labeling methodology for expression profiling. RT: reverse transcription; Bi: biotin; blue and green arrows: primers. **(B)** Multiple harvests of MEP (n=8), MEGA1 (n=4), MEGA2 (n=6), ERY1 (n=4), ERY2 (n=3), and ERY3 (n=2) populations were purified from human umbilical cord blood cells (Experimental Procedures) and profiled for miRNA expression. A heatmap is shown for log2-transformed data, with red color indicating higher expression and blue for lower expression. Data reflect the median expression of miRNAs within corresponding populations. Arrows point to miRNAs mentioned in text. **(C)** Median expression of miR-150 was plotted for each

population, with the oval area proportional to the expression level. **(D)** miR-150 expression was measured using quantitative RT-PCR on multiple harvests of MEP (n=3), MEGA1 (n=4), MEGA2 (n=3), ERY1 (n=3), ERY2 (n=3) and ERY3 (n=3) populations. The ΔCt values (Ct (threshold cycle) of 18S minus Ct of miR-150) are shown for all samples. Note that ΔCt reflects log scale of expression. Samples indicated with black dots were also used in miRNA profiling in (B) and (C), whereas those with red circles were additional samples. **(E)** Megakaryocytes ($CD41^+CD61^+$) and erythrocytes ($CD71^+GlyA^+$) were FACS-sorted from the bone marrow of a healthy adult human donor. miR-150 expression was measured using quantitative RT-PCR. Data reflect $2^{\Delta Ct}$ in arbitrary units (AU) Error bars represent standard deviation.

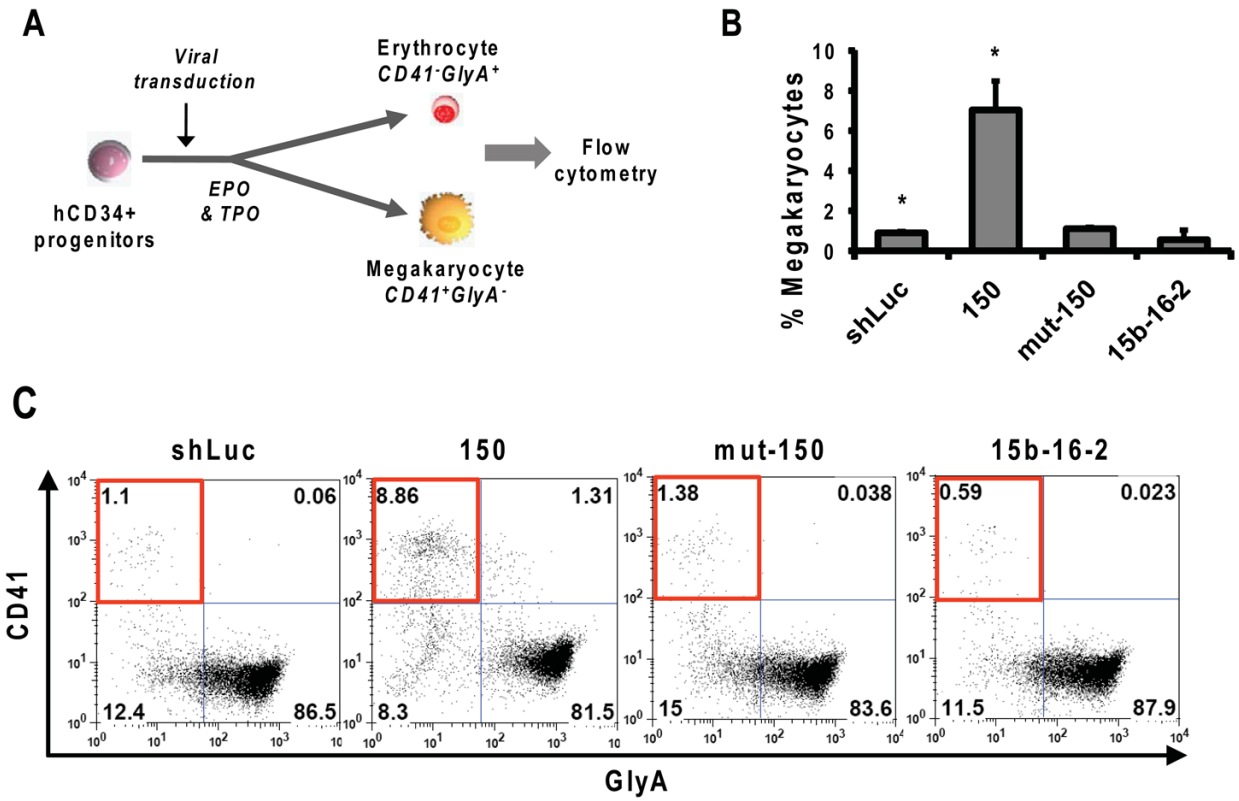

Figure 2. miR-150 regulates megakaryocyte and erythrocyte development *in vitro*.

(A) The function of miR-150 was assayed in an *in vitro* primary culture. CD34+ hematopoietic progenitors derived from human adult bone marrow cells were transduced with viral constructs expressing a control hairpin (shLuc), miR-150, a mutant miR-150 or miR-15b-16-2. The cells were cultured in the presence of erythropoietin (EPO) and thrombopoietin (TPO) to differentiate toward erythrocytes and megakaryocytes, and were analyzed after 10 days of differentiation, using flow cytometry with lineage markers CD41 (megakaryocytic) and GlyA (erythroid). **(B)** The effect of the expression constructs on the percentage of megakaryocytes ($CD41^+GlyA^-$) is shown. The data reflect a representative triplicate experiment. Error bars represent standard deviation. * $P<0.03$. **(C)** Representative flow cytometry plots are shown.

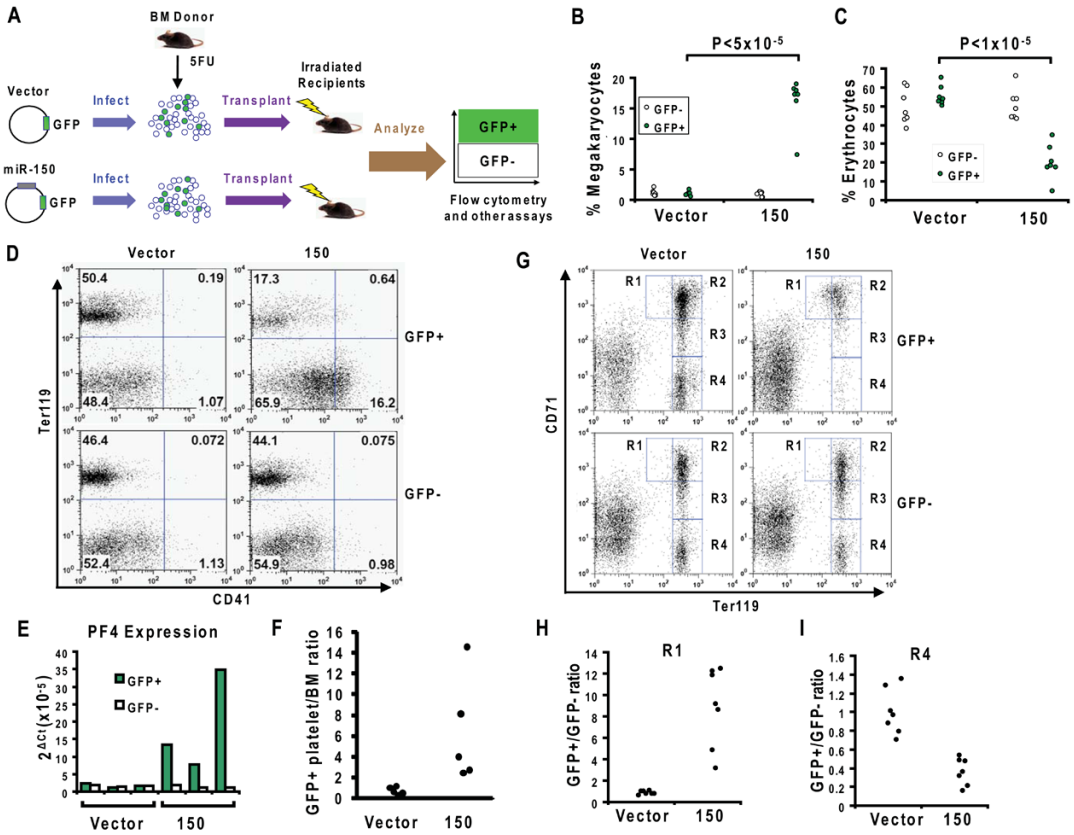

Figure 3. miR-150 reciprocally regulates megakaryocyte and erythrocyte development *in vivo*

(A) The function of miR-150 was assayed in a murine transplant model. Stem/progenitor-cell-enriched bone marrow cells from donor mice were transduced with a control vector or a miR-150 expression construct. The vectors carry a GFP marker, thus labeling transduced cells and cells derived from them with green fluorescence. The mixture of transduced and non-transduced donor cells was transplanted into lethally irradiated recipients. Bone marrow and peripheral blood of recipients were analyzed 5 to 8 weeks post transplantation, when the hematopoietic system had largely recovered in the hosts. **(B)** The percentage of recipient bone marrow GFP^+ or GFP^- megakaryocytes ($CD41^+Ter119^-$) is shown. Each dot represents data from one recipient mouse. n=7. **(C)** Bone marrow GFP^+ or GFP^- erythrocyte ($CD41^-Ter119^+$) percentage is shown. n=7. **(D)** Representative flow cytometry plots on bone marrow cells with megakaryocytic (CD41) and erythroid (Ter119) markers. **(E)** Recipient bone marrow cells were FACS-sorted into GFP^+ and GFP^- populations, and measured for PF4 expression using quantitative RT-PCR. Each pair of bars represents data from one recipient mouse. **(F)** The circulating platelets were analyzed in the peripheral blood of recipient animals. The ratio of GFP^+ platelet percentage to the percentage of GFP^+ bone marrow cells was plotted to reflect the thrombocytogenic potential of transduced bone marrow cells. n=5. **(G)** Representative flow cytometry plots of bone marrow cells assayed with CD71 and Ter119. The gates R1 to R4 represent immature to mature erythrocytes. **(H)** The percentage of R1 population among all erythrocytes (sum of R1 to R4) was used to derive a ratio between GFP^+ and GFP^- population within the same recipient mouse. n=7. $P<0.002$. **(I)** Data for R4 population, similarly derived as in (I). $P<2\times10^{-4}$.

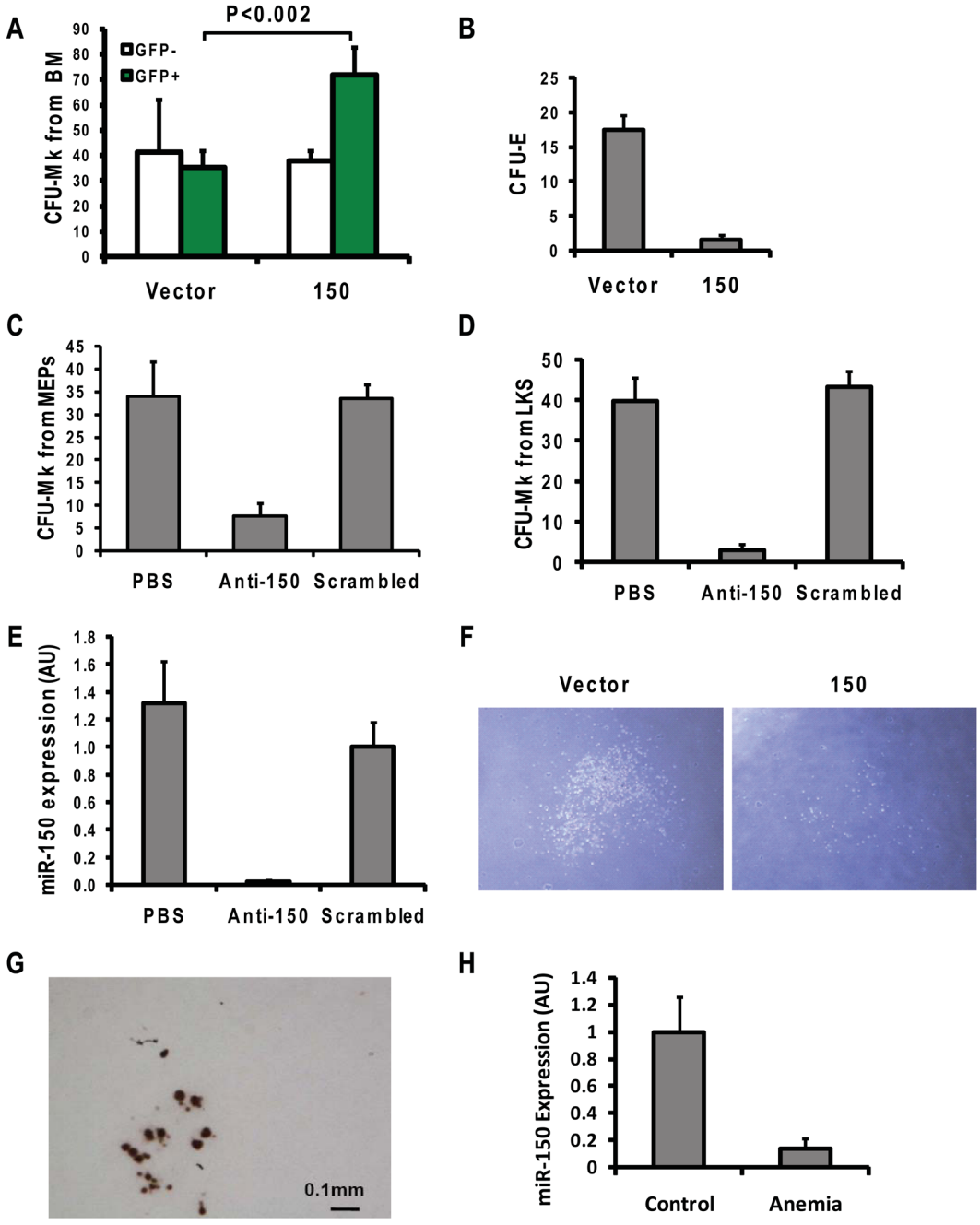

Figure 4. miR-150 regulates lineage fate in MEPs

(A) Bone marrow cells from vector control or miR-150 recipient animals were sorted into GFP + and GFP− populations. Megakaryocyte colony forming units (CFU-Mks) were quantitated from 100,000 sorted cells. n=4. **(B)** Bone marrow cells from 5FU treated mice were transduced with a control vector or miR-150 and 30,000 transduced bone marrow cells were assayed for erythroid colony forming units (CFU-E). **(C)** MEP cells sorted from wild-type C57BL/6J mice were assayed for CFU-Mk in the presence of PBS (vehicle), antagomir against miR-150 (anti-150) or a scrambled antagomir. 4000 cells were analyzed per assay. n=4. **(D)** $Lin^{-}Kit^{+}Sca^{+}$ (LKS) stem cells were assayed as in (B). 1000 cells were analyzed per assay. n=4. **(E)** The expression of miR-150 in murine bone marrow cells was measured with

quantitative RT-PCR after 3 days of treatment of PBS or antagomirs. Data reflect $2^{\Delta Ct}$ in arbitrary units (AU). Error bars represent standard deviation. **(F)** Representative erythroid colonies from control-vector- or miR-150-transduced bone marrow cells. Note that rare erythroid colonies formed from miR-150 transduced cells showed reduced cell number. **(G)** A representative megakaryocyte colony grown in the presence of antagomir-150 is shown. Brown color reflects megakaryocyte-specific acetylcholinesterase activity. **(H)** Mice were treated with PBS (control) or with phenylhydrazine to induce anemia. miR-150 expression was assayed by quantitative RT-PCR in lineage negative cells purified from bone marrow. n=3. $P<0.001$. Error bars represent standard deviation.

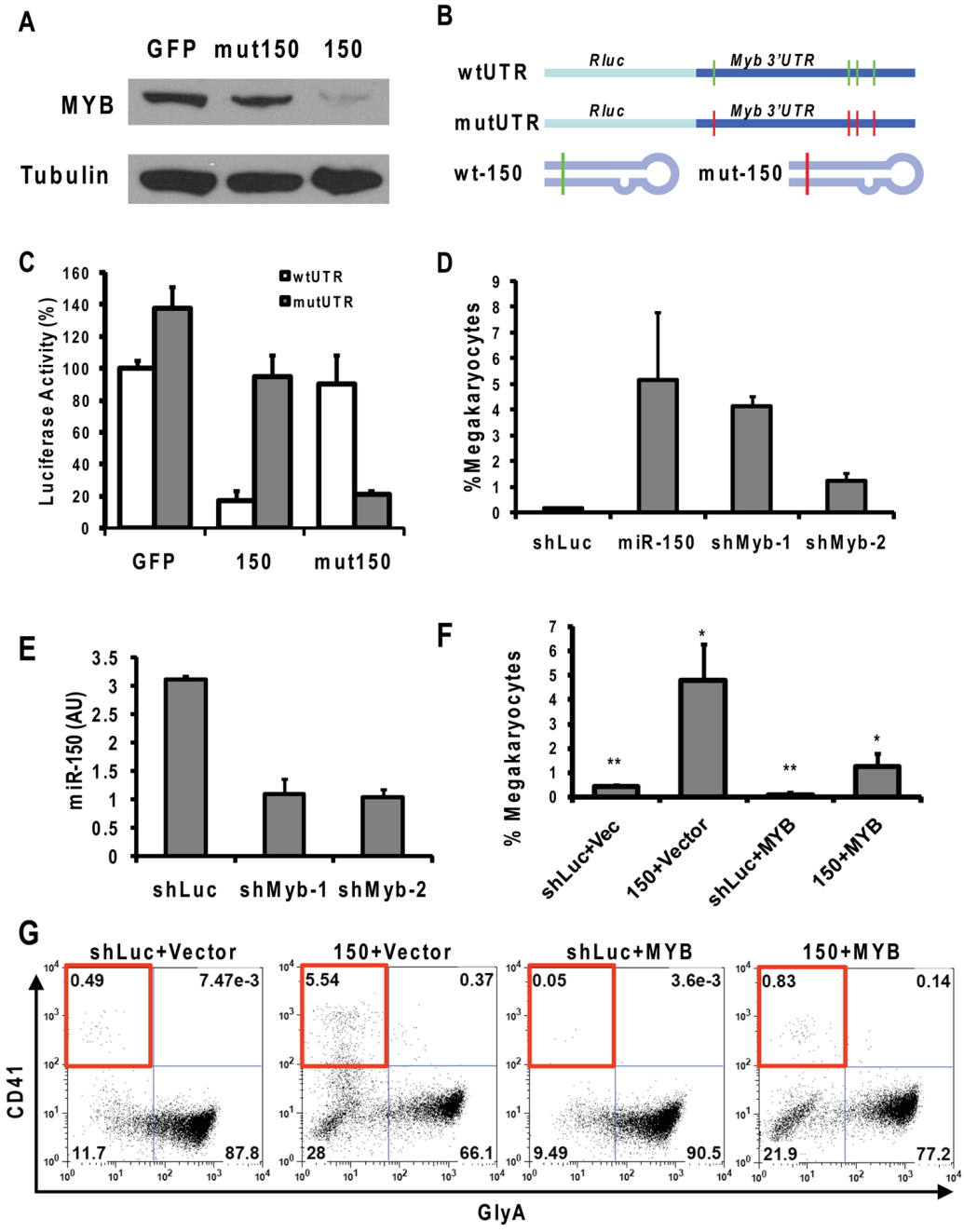

Figure 5. *MYB*is a direct and functional target of miR-150

(A) K562 cells were transduced with constructs expressing GFP, mutant miR-150 or miR-150, and assayed for *MYB* and beta-Tubulin with western blot analysis. **(B)** Design of luciferase reporters for human *MYB* 3′ UTR, with green vertical bar indicating wild-type (wt) sites and red indicating mutant (mut) sites. The mutant miRNA site and mutant 3′UTR sites are complementary. **(C)** Normalized luciferase activities in 293T cells. Error bars represent standard deviation. n=8. **(D)** CD34+ human adult bone marrow cells were transduced with control vector (shLuc), miR-150 or two independent shRNAs against *MYB* in an *in vitro* culture as described in Figure 2. The percentage of megakaryocytes ($CD41^{+}GlyA^{-}$) was measured by flow cytometry. A representative triplicate experiment is shown. **(E)** The knockdown of

MYB by shRNAs was measured in K562 cells, as determined by quantitative RT-PCR. The values reflect $2^{\Delta Ct}$ in arbitrary units (AU). **(F)** miR-150 and *MYB* expression constructs and their corresponding vector controls (shLuc, Vector) were assayed in combination in the human $CD34^{+}$ cell culture. A representative triplicate experiment is shown. * P=0.04; ** P<0.01. **(G)** Representative flow cytometry plots as described in (F). Error bars in all panels represent standard deviation.